Supplementary Materials for

Sexually Dimorphic BDNF Signaling Directs Sensory Innervation of the Mammary Gland

Yin Liu, Michael Rutlin, Siyi Huang, Colleen A. Barrick, Fan Wang, Kevin R. Jones, Lino Tessarollo, David D. Ginty*

*To whom correspondence should be addressed. E-mail: dginty@jhmi.edu

Published 7 December 2012, *Science* **338**, 1357 (2012)
DOI: 10.1126/science.1228258

This PDF file includes

Materials and Methods

Embryo stages

The day on which vaginal plug was observed after setting up matings was counted as embryonic day 0. Stages of embryos were further confirmed by checking embryo morphology and limb development (*23*). Embryos were collected at two different times at a given embryonic day: 9-10am was considered as early of that day, and 4-5pm was considered as late of that day.

Genotyping protocol for determining sex

Primers for genotyping the Zfy1 gene are: 5'-ACATGGAGAGCCACAAGCTAACCA-3' and 5'-CTTTCTTGGTGCAGAACGGCATGT-3'. The size of the PCR product from male embryos is 468bp.

Mouse lines

The androgen-insensitive *Tfm (10)*, *Avil*^{Cre} *(22)*, *BDNF*^{LacZ} *(21)*, *TrkB.T1 (20)*, and *TrkB*^{GFP} *(13)* (previously referred to as *TrkB*^{tauEGFP}) mice have been described previously. The targeting vector used to generate the *NGF*^{LacZ} knock-in allele and the embryonic stem (ES) cells used to generate the *NT-4*^{LacZ} knock-in allele were obtained from EUCOMM. Generation of mice harboring the *TrkB*^{CreERT2} allele will be described elsewhere. The *TrkB*^{f} and *TrkB*^{F616A} mice were modified versions of the TrkB chemical-genetic mice described previously *(14)*. For the *TrkB*^{f} allele, a 3.2 kb sequence containing exon 15 and a FRT-Neo-FRT cassette was flanked by two loxP sites. For the *TrkB*^{F616A} allele, the same 3.2 kb sequence containing exon 15, but lacking loxP sites, harbors the F616A

mutation. Homologous recombination for both targeting constructs was performed using 129.1 mouse strain embryonic stem (ES) cells. ES cell clones that exhibited homologous recombination were screened by PCR, and results were confirmed by Southern blotting. Correctly targeted ES clones were injected into C57BL/6 blastocysts, which were then introduced into pseudopregnant females. Heterozygous mice were generated by crossing chimeric mice with C57BL/6 mice, and these mice were subsequently crossed with mice expressing FlpE recombinase in germ cells to excise the *Neo* cassette. Both lines were backcrossed and maintained on a C57BL/6 background. Mice were genotyped using PCR reactions with following primers: 5'-GGGCTTGAGAAGAGGGCAAAAGGGTTGCTCAG-3' and 5'-GTTGGTCACCAGCAGAACACTCGACTCAC-3'. The sizes of PCR products of the wildype, $TrkB^{f}$, and $TrkB^{F616A}$ alleles are 280bp, 430bp, and 350bp, respectively.

Drug treatments

Flutamide (Sigma F9397) was dissolved in DMSO to make a 500mg/ml stock, and 20µl of this stock solution or DMSO diluted with 500µl sunflower seed oil was delivered to pregnant females by oral gavage at E12 (5-6pm) and E13 (10-11am). Testosterone propionate (Sigma T1875) was dissolved in sunflower seed oil to make a 20mg/ml solution, and 50µl of this solution or sunflower seed oil was delivered to the pregnant females by subcutaneous injections. DHT was dissolved in ethanol to make a 50mg/ml solution, right before use 20µl of this solution was mixed well with 60µl sunflower seed oil, and vacuum centrifuged to evaporate the ethanol before subcutaneous injections. For 1NMPP1/$TrkB^{F616A}$ chemical-genetic experiments, the $TrkB^{F616A}$ inhibitor 1NMPP1

was dissolved in DMSO to make a 200mM stock, and 2.5µl of the 1NMPP1 stock solution or DMSO was diluted into 100µl of injection solution (0.9% NaCl, 2.5% Tween-20) for subcutaneous injections. For oral gavage administration, 0.5µl 1NMPP1 stock solution or DMSO was diluted into 20ul of injection solution and then further diluted into 500µl water. Treatments were given every 1.5hr, four times, beginning at E13 (11am). The inhibitor 1NMPP1 was synthesized by *Aurora Analytics, LLC*, as previously described (*24*).

Immunohistochemistry

Embryonic tissues were fixed in PBS containing paraformaldehyde (PFA, 4%) at 4°C for 2 hours to overnight, followed by cryoprotection at 4°C in PBS containing 30% sucrose. P3 mammary glands were dissected together with fat pads and adjacent skin, fixed in 4% PFA in PBS at 4°C for 1-2hr, and cryoprotected in 30% sucrose in PBS at 4°C. Tissues were embedded in OCT (Tissue Tek), frozen at -20°C, and sectioned at 20µm. Tissue sections were dried overnight at room temperature, washed with PBS and blocked with 5% normal serum (goat or donkey) in PBST (0.1% Triton X-100 in PBS) for 30min, followed by primary antibody incubation (diluted in blocking solution) overnight at 4°C. The next day, sections were washed with PBST, and incubated with secondary antibodies diluted in blocking solution for 1-2hrs, washed again with PBST, and mounted with fluoromount-G (Southern Biothech). Pictures were taken using a Carl Zeiss LSM700 laser scanning microscope. Primary antibodies used for immunohistochemistry were: Androgen receptor (Invitrogen, 1:300), DsRed (Clontech, 1:500), GFP (Aves Lab, 1:500), $TrkB^{ECD}$ (R&D, 1:100), the truncated form of TrkB (Santa Cruz, 1:50), Tuj1

(Covance, 1:1000). The nucleic acid stain TO-PRO-3 (Invitrogen 1:500) was applied along with secondary antibody incubation during immunohistochemistry.

In situ hybridization

Protocols for *in situ* hybridization were described previously (*25*). Embryos were fixed in 4% PFA in PBS at 4°C for overnight, and cryoprotected in 30% sucrose in PBS at 4°C. Tissues were embedded in OCT (Tissue Tek) and frozen at -20°C. Tissue sections were cut at 14-20μm and then dried at room temperature for 1hr. The probe for full-length *TrkB* was generated to detect an 842bp sequence in the 3'UTR of full-length TrkB mRNA (NM_001025074.1). Primers for generating this probe construct were: 5'-ATGAGCGAGACAGAGACAAGCCAT-3' and 5'-ACCTTGGAATGAAACCACTCTCCC-3'. The probe for both forms of TrkB was generated to detect an 853bp sequence in the coding region for the extracellular domain of TrkB. Primers for generating this probe construct were: 5'-AATGAGAGCAGCAAGAACATGCCC-3' and 5'-GCCAAACTTGGAATGTCTCGCCAA-3'. Probes were labeled with Dioxygenin (DIG).

X-gal staining

Embryos were fixed with a glutaraldehyde solution (0.2% glutaraldehyde, 2mM $MgCl_2$ in PBS) overnight at 4°C. For whole-mount staining, fixed embryos were washed with detergent rinse buffer (0.01% sodium deoxycholate, 0.02% NP40, 2mM $MgCl_2$ in phosphate buffer, pH 7.4), and stained with staining buffer (0.01% sodium deoxycholate,

0.02% NP40, 2mM $MgCl_2$, 5mM potassium ferricyanide, 5mM potassium ferrocyanide, 1mg/ml 5-bromo-4-chloro-indolyl-β-D-galactopyranoside in phosphate buffer, pH 7.4) at room temperature. After staining, embryos were dehydrated sequentially with 50% methanol, 80% methanol, and 100% methanol. For staining on sections, 12μm sections were cut and dried for several hours at room temperature. The staining procedure was the same as described for whole-mount staining. After staining, sections were fixed overnight at 4°C in 4% PFA in PBS, and mounted with fluoromount-G.

Carmine staining and alkaline phosphatase histochemistry on whole-mount mammary glands

Whole mount carmine staining and placental alkaline phosphatase (AP) staining were carried out by procedures described previously (*26, 27*). P0 mammary glands were dissected with fat pads intact, and fixed in 4% PFA in PBS at 4°C for 1hr. To reveal the gland ductal tree structure, fixed mammary glands were stained with carmine aluminum (Sigma C1022) solution overnight at room temperature, dehydrated with 50%, 75%, 95%, 100% ethanol, and cleared in xylene. To detect the PLAP signal, fixed mammary glands were stained with BCIP/NBT (Roche) solution overnight at room temperature, followed by post-fixation in 4% PFA in PBS overnight at 4°C, dehydrated with 50%, 80%, 100% methanol, and cleared in BABB.

Fig. S1

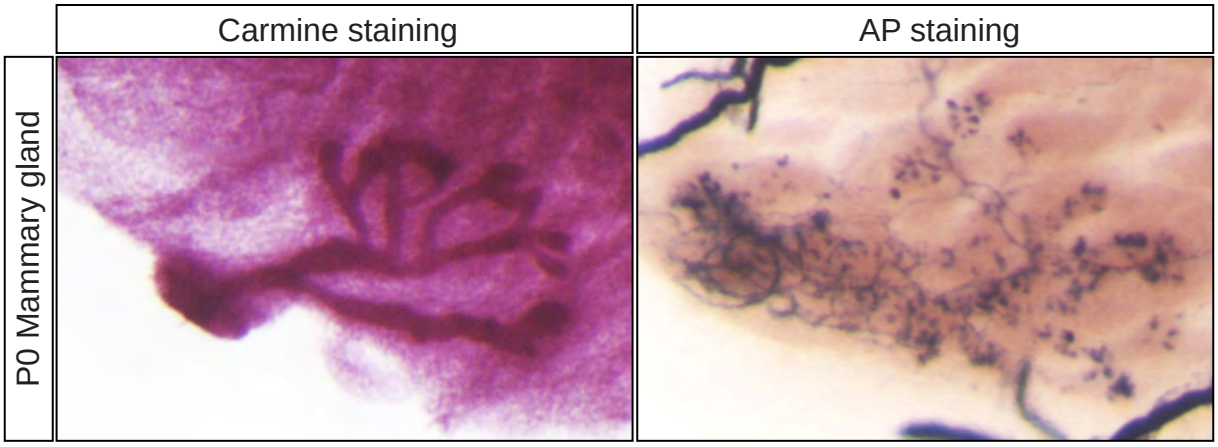

Fig. S1. The mammary gland ductal tree is densely innervated by sensory fibers at P0. Mammary glands were dissected from a P0 *Advillin-hPLAP* female mouse in which placenta alkaline phosphatase is expressed exclusively in primary sensory neurons (*28*). The ductal tree structure is revealed by Carmine staining (left panel), and sensory innervation of the mammary gland is shown by alkaline phosphatase histochemistry (right panel). This experiment was done two times with similar results.

Fig. S2

A

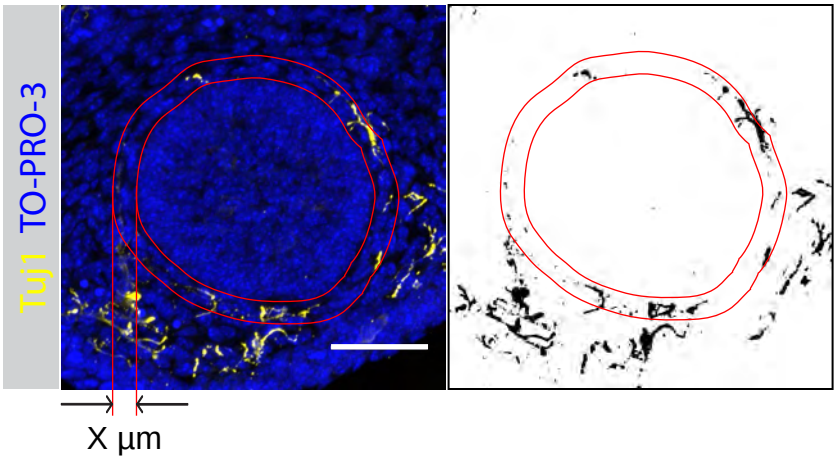

$$\text{Fiber density (\%)} = \frac{\text{Area of Tuj1 staining within the band}}{\text{Total area of X µm band surrounding the mammary rudiment}} \times 100\%$$

B

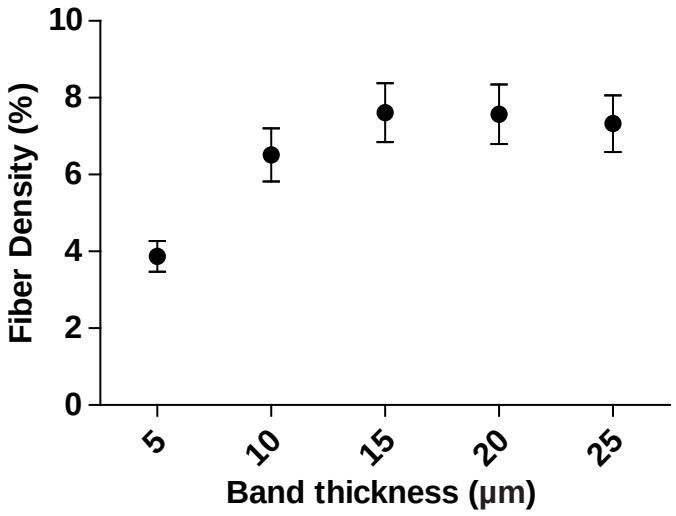

Fig. S2. Quantification of neuronal fibers projecting to the rudimentary mammary gland. For all experiments, images were processed and analyzed using ImageJ software. (**A**) Mammary gland cross sections were stained with anti-Tuj1 and TO-PRO-3. The edge of the rudimentary mammary gland was determined by TO-PRO-3 staining, and a band with the indicated thickness (X) surrounding the gland was drawn automatically with ImageJ. The total number of Tuj1 positive pixels within this band was counted, divided by the total number of pixels occupied by the entire band area, and this number was multiplied by 100% to obtain the measurement of fiber density. (**B**) Average fiber densities of different band thicknesses (20 rudimentary mammary glands from 4 late E13 female embryos, mean ± s.e.m.). Since the fiber density peaks for measurements using the 15 μm band, all subsequent quantifications presented in this study use 15 μm as the band thickness.

Fig. S3

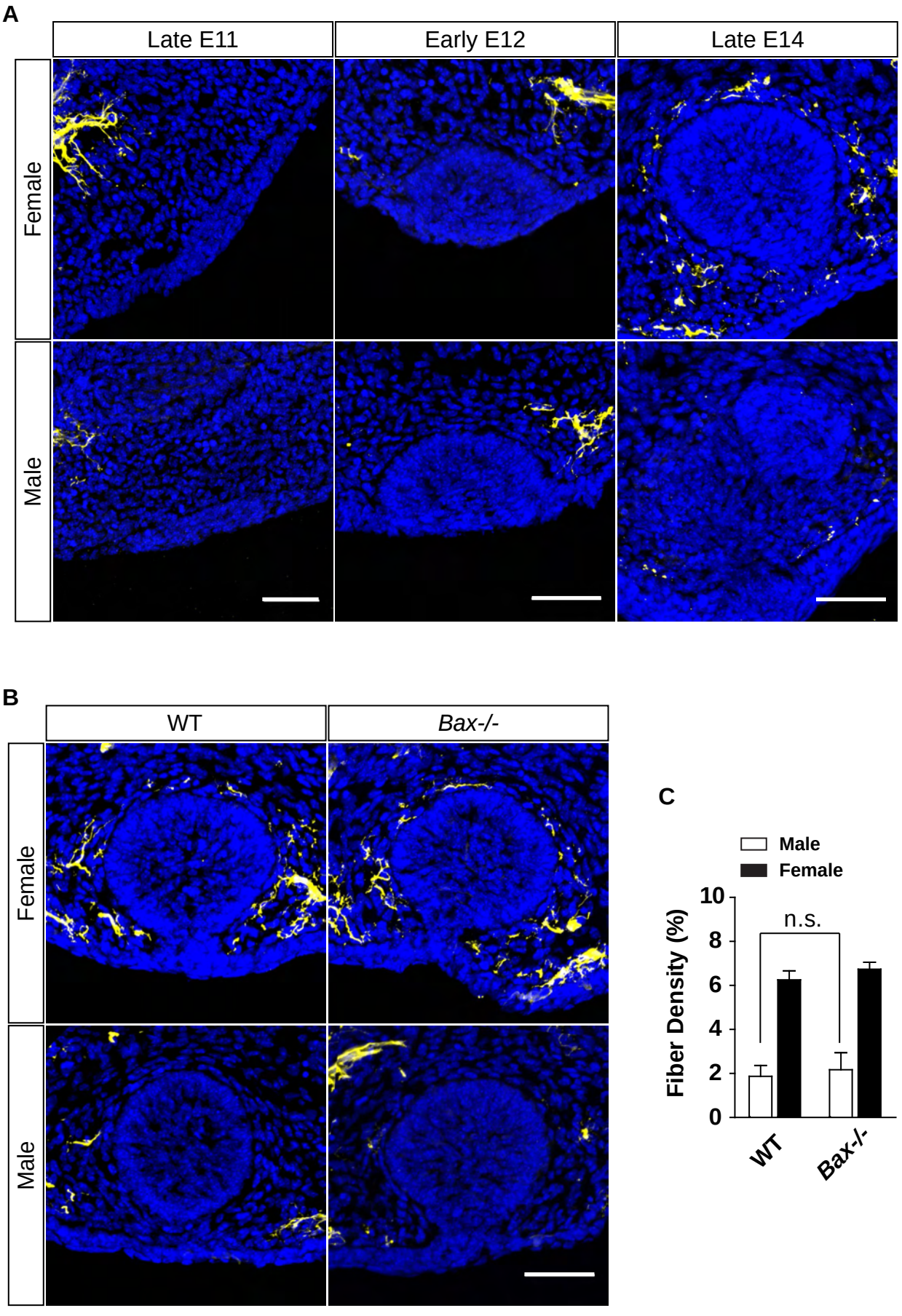
A
Late E11
Early E12
Late E14
Female
Male
B
WT
Bax-/-
Female
Male
C
Male
Female
Fiber Density (%)
10
8
6
4
2
0
n.s.
WT
Bax-/-

Fig. S3. Sexually dimorphic mammary gland innervation is independent of apoptotic cell death. (**A**) Tuj1 and TO-PRO-3 staining of mammary gland sections at late E11, early E12, and late E14. Mammary rudiments first appear as thickening of the epithelium at late E11, and then become bud-shape at early E12. Note that neuronal fibers reach mammary rudiments after early E12. (**B**-**C**) Mammary gland innervation of late E13 wildtype and *Bax*-/- embryos (n≥3 embryos for each bar). Scale bar: 50μm.

Fig. S4

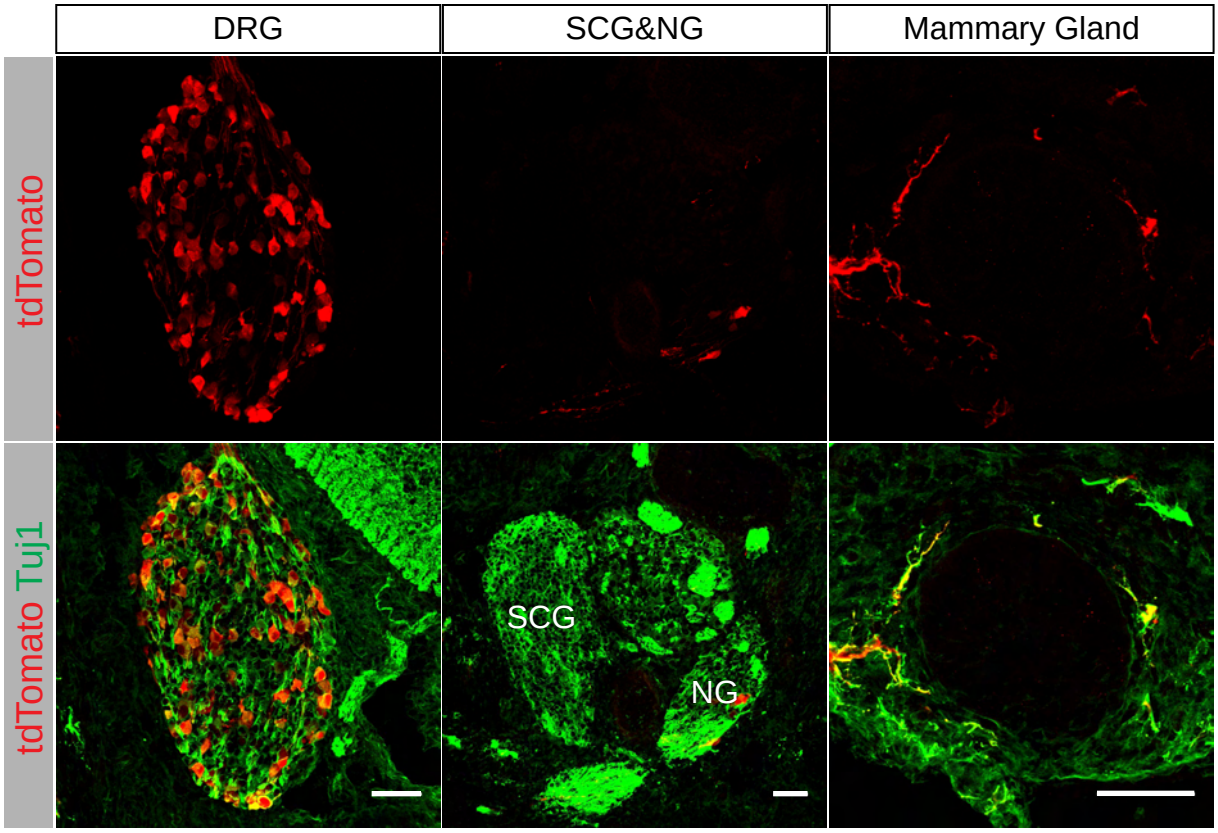

Fig. S4. Neuronal fibers innervating the E13 rudimentary mammary glands emanate from sensory ganglia. The *Avil*^{Cre} mouse line was crossed with a Cre recombinase dependent *Rosa26*^{LSLtdTomato} reporter line (*29*) to specifically label sensory neurons. E13 female *Avil*$^{Cre/+}$; *Rosa26*$^{LSLtdTomato/+}$ embryos were analyzed, and cross-sections of dorsal root ganglia (DRG), sympathetic ganglia (SG), nodose ganglia (NG), and rudimentary mammary glands were stained with anti-DsRed (to detect tdTomato) and anti-Tuj1. There are many tdTomato^{+} neurons in the DRG while very few neurons are found to express tdTomato in the NG. Labeled neurons were not observed in the SG (a section through the superior cervical ganglion (SCG) is shown in the figure). All Tuj1^{+} fibers surrounding rudimentary mammary glands are tdTomato positive, indicating that they are from sensory neurons, most likely DRG sensory neurons. This experiment was done two times with similar results. Scale bar: 50μm.

Fig. S5

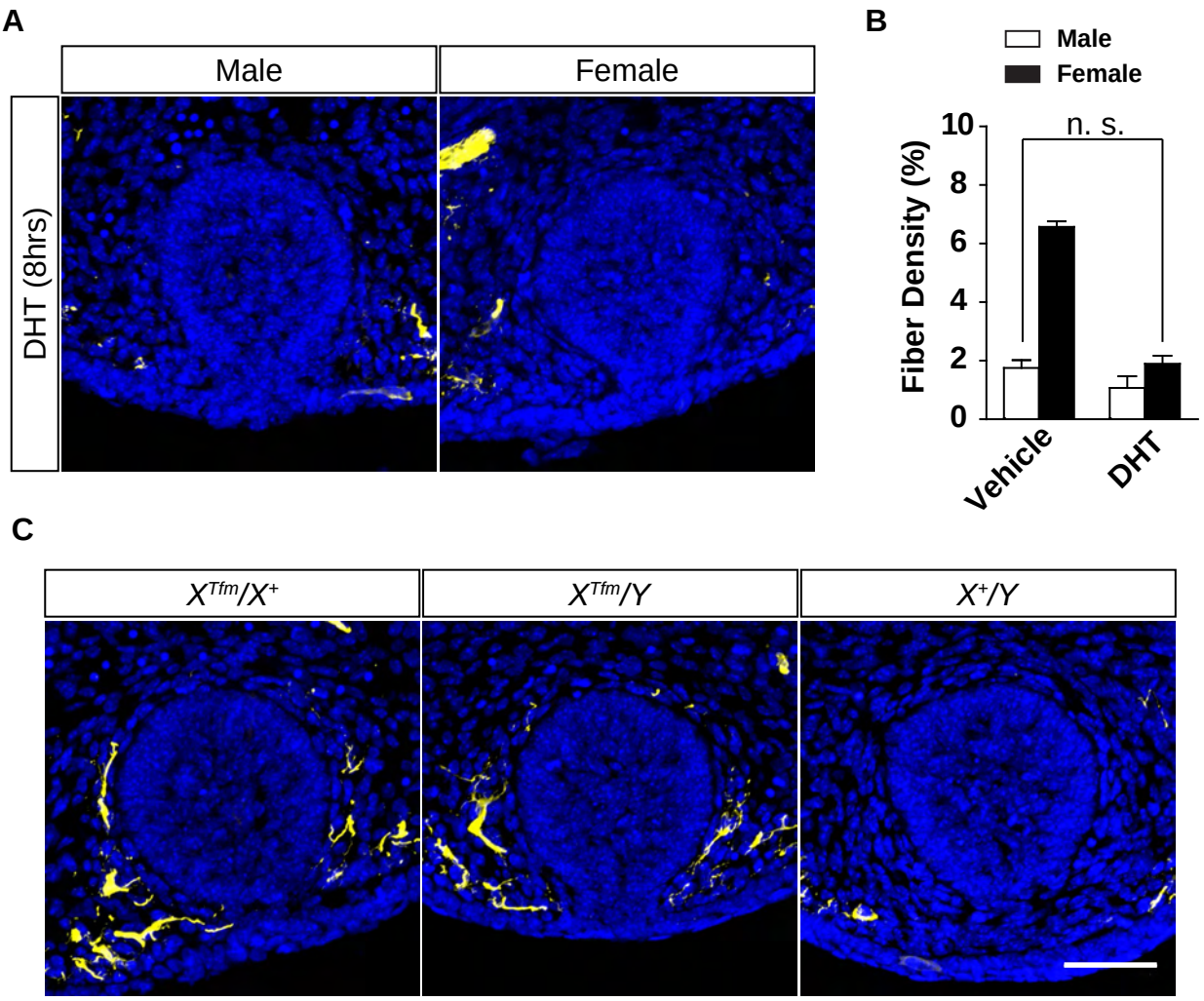

Fig. S5. Sexually dimorphic mammary gland innervation is dependent on androgen receptor activation. (**A**) Pregnant dams were treated with 1mg DHT by subcutaneous injection 8 hours prior to sacrifice, and embryos were collected at late E13. Mammary gland sections were stained with anti-Tuj1 and TO-PRO-3. (**B**) Quantification of mammary gland innervation (n≥3 embryos for each bar). The vehicle group is the same vehicle group for the testosterone treatments, shown in fig. 1. (**C**) Mammary gland innervation of heterozygous *Tfm* female, hemizygous *Tfm* male, and wildtype male embryos at late E13. This experiment was done two times with similar results. Scale bar: 50μm.

Fig. S6

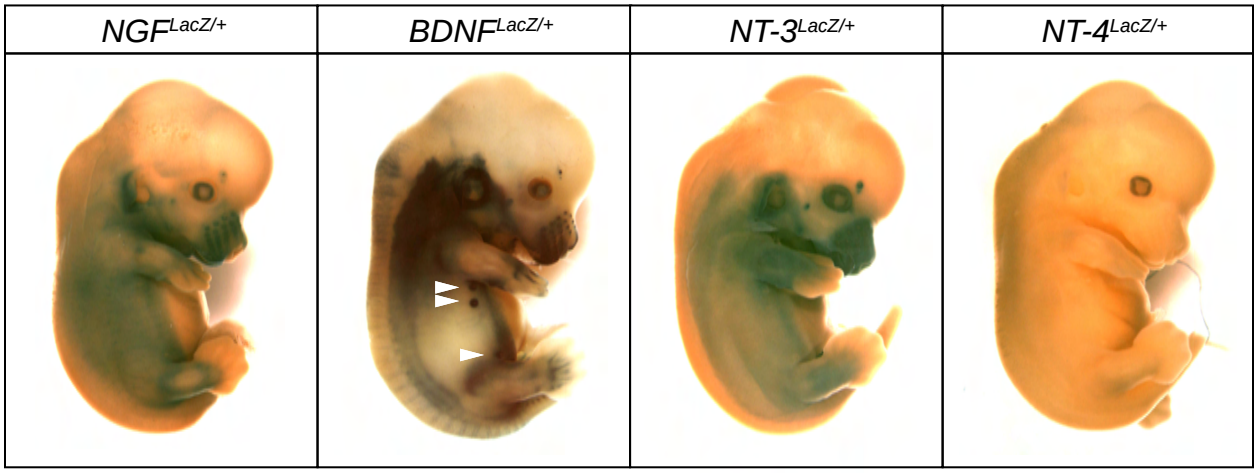

Fig. S6. NGF, BDNF, NT-3, and NT-4 expression patterns in E13 mouse embryos. Whole-mount X-gal staining of E13 female *NGF*$^{lacZ/+}$, *BDNF*$^{LacZ/+}$, *NT-3*$^{LacZ/+}$ *(30)*, and *NT-4*$^{LacZ/+}$ embryos. Staining associated with E13 mammary glands is only detected in *BDNF*$^{LacZ/+}$ embryos Arrows: rudimentary mammary glands (five on each side of the body; glands #1 and #5 are behind the limbs and therefore not seen in this image). Staining of each mouse line was done at least two times with similar results.

Fig. S7

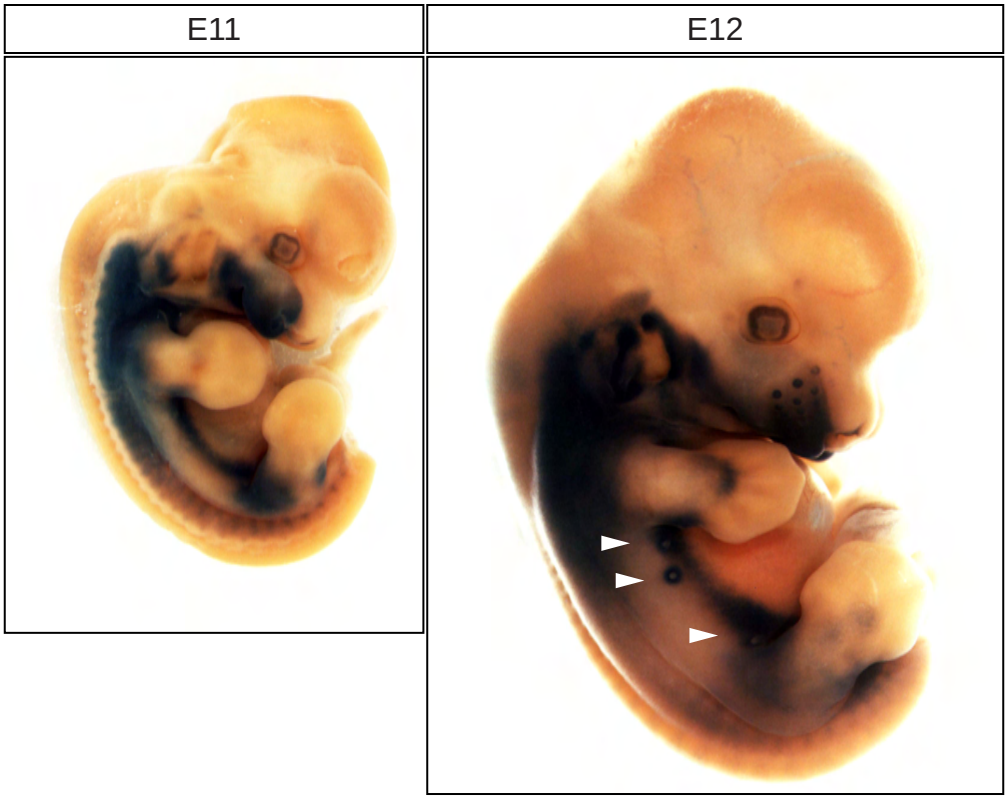

Fig. S7. The BDNF expression pattern in E11 and E12 *BDNF*$^{LacZ/+}$ mouse embryos. Whole-mount X-gal staining of *BDNF*$^{LacZ/+}$ embryos at E11 and E12. LacZ expression is associated with the developing mammary glands beginning at E12. Staining was done for mice at each time point at least two times with similar results.

Fig. S8

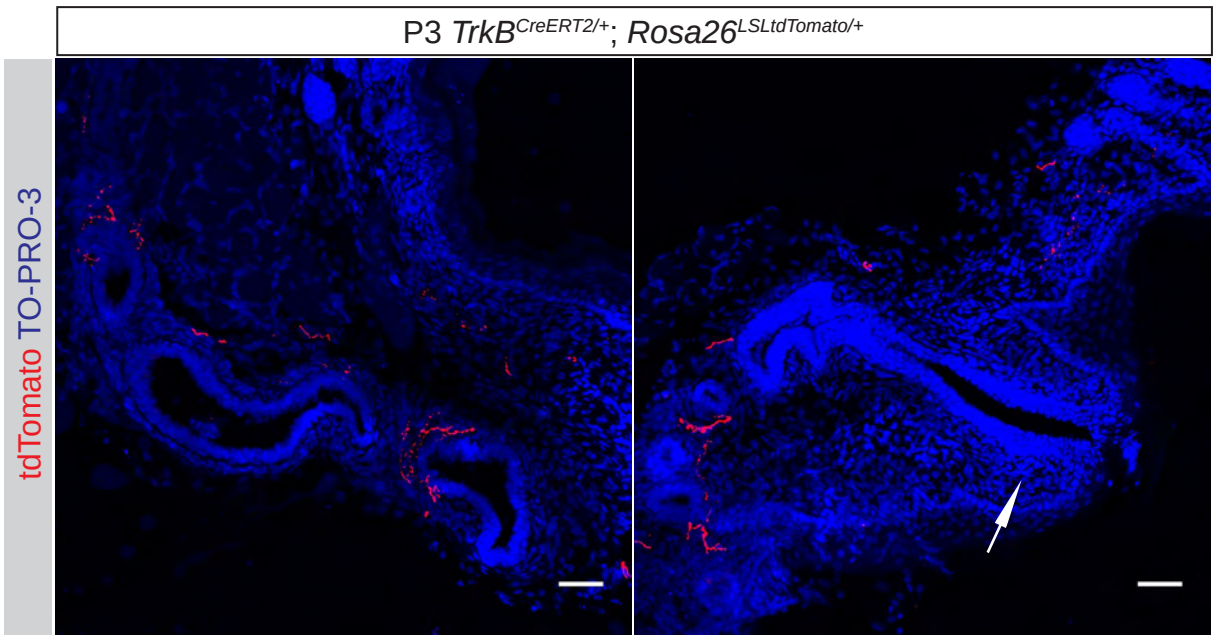

Fig. S8. Neurons expressing TrkB at E13 innervate the mammary gland ductal tree structure but not the nipple in postnatal female mice. The *TrkB*^{CreERT2} mouse line was crossed with a *Rosa26*^{LSLtdTomato} reporter line and the pregnant females were treated with 4mg tamoxifen at E13 (11am) by oral gavage. *TrkB*$^{CreERT2/+}$*; Rosa26*$^{LSLtdTomato/+}$ females were sacrificed at P3, and isolated mammary glands with nipples and surrounding skin were obtained. Cross-sections of mammary glands were stained with anti-DsRed and TO-PRO-3 (sections shown here are from two different mammary glands). All tdTomato positive fibers associated with the mammary glands innervate the ductal structure, but not the nipples (arrow points to the nipple region). This experiment was done two times with similar results. Scale bar: 50μm.

Fig. S9

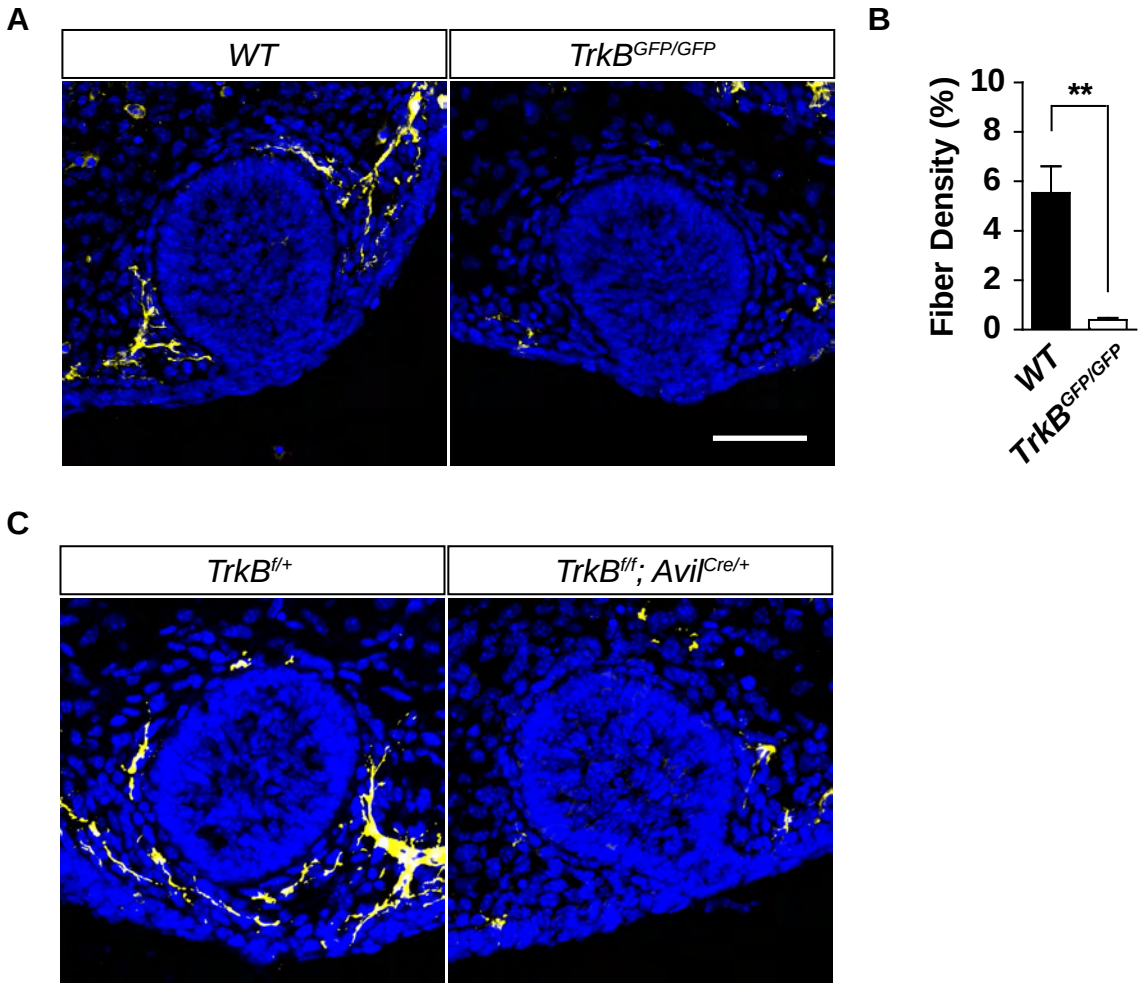

Fig. S9. TrkB is required in sensory neurons for the establishment of female mammary gland innervation. (**A-B**) Mammary gland innervation of late E13 female wildtype and *TrkB*$^{GFP/GFP}$ (null) embryos (n≥3 embryos for each bar). (**C**) Mammary gland innervation of late E13 female *TrkB*$^{f/+}$ and *TrkB*$^{f/f}$*; Avil*$^{Cre/+}$ (sensory neuron-specific *TrkB* deletion) embryos. Quantification of these data is shown in fig. 2F. Scale bar: 50μm.

Fig. S10

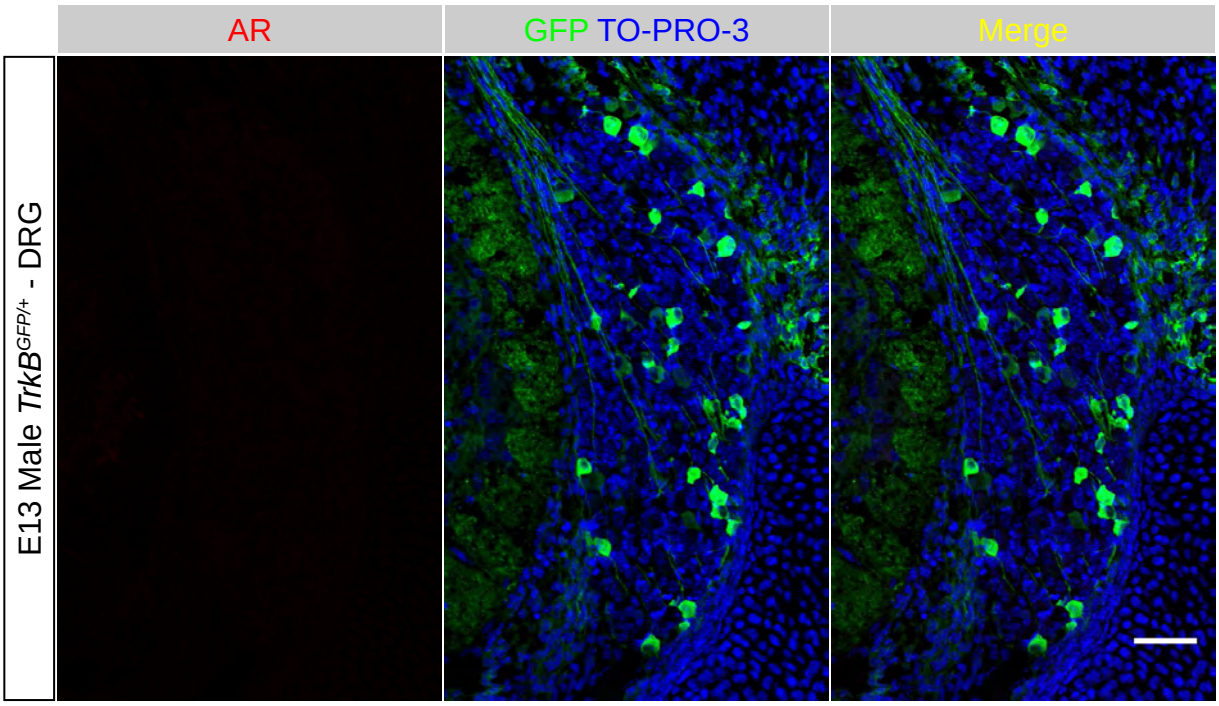

Fig. S10. The androgen receptor is not expressed in DRG neurons at E13. An E13 male DRG section was stained with an androgen receptor antibody (AR), and co-stained with anti-TrkB^{ECD} and TO-PRO-3. A similar pattern was observed in sections of female DRGs (not shown). This experiment was done three times with similar results. Scale bar: 50µm.

Fig. S11

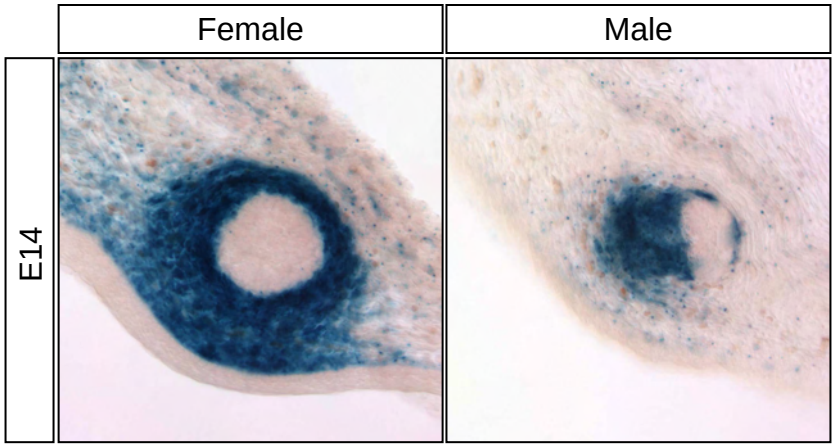

Fig. S11. BDNF expression in E14 male and female mammary mesenchyme. X-gal staining on cross-sections of mammary rudiments of *BDNF*$^{LacZ/+}$ male and female embryos at early E14. At this stage, male mammary glands are in regression, with both mammary mesenchymal cells and mammary epithelial cells undergoing apoptosis.

Fig.S12

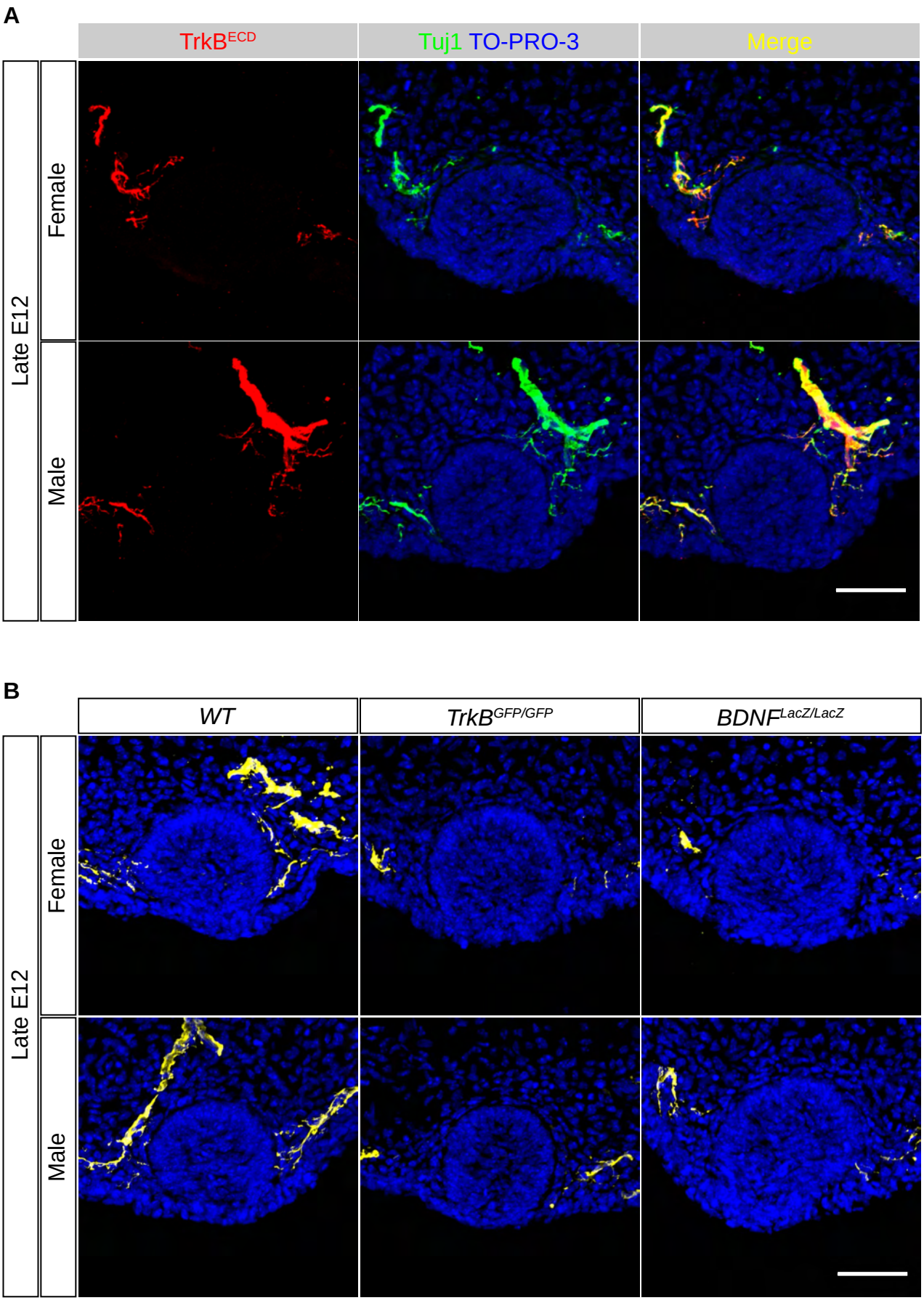
A
TrkB^ECD
Tuj1 TO-PRO-3
Merge
Late E12
Female
Male
B
WT
TrkB^GFP/GFP
BDNF^LacZ/LacZ
Late E12
Female
Male

Fig. S12. BDNF-TrkB signaling is required for initial axonal projections to both the male and female mammary glands. (**A**) Embryos were collected at late E12 and sections of both male and female rudimentary mammary glands were stained with anti-TrkB^{ECD}, anti-Tuj1 and TO-PRO-3. (**B**) Mammary gland innervation of wildtype, *TrkB*$^{GFP/GFP}$, and *BDNF*$^{LacZ/LacZ}$ embryos at late E12 (stained with anti-Tuj1 and TO-PRO-3). These experiments were done two times with similar results. Scale bar: 50μm.

Fig. S13

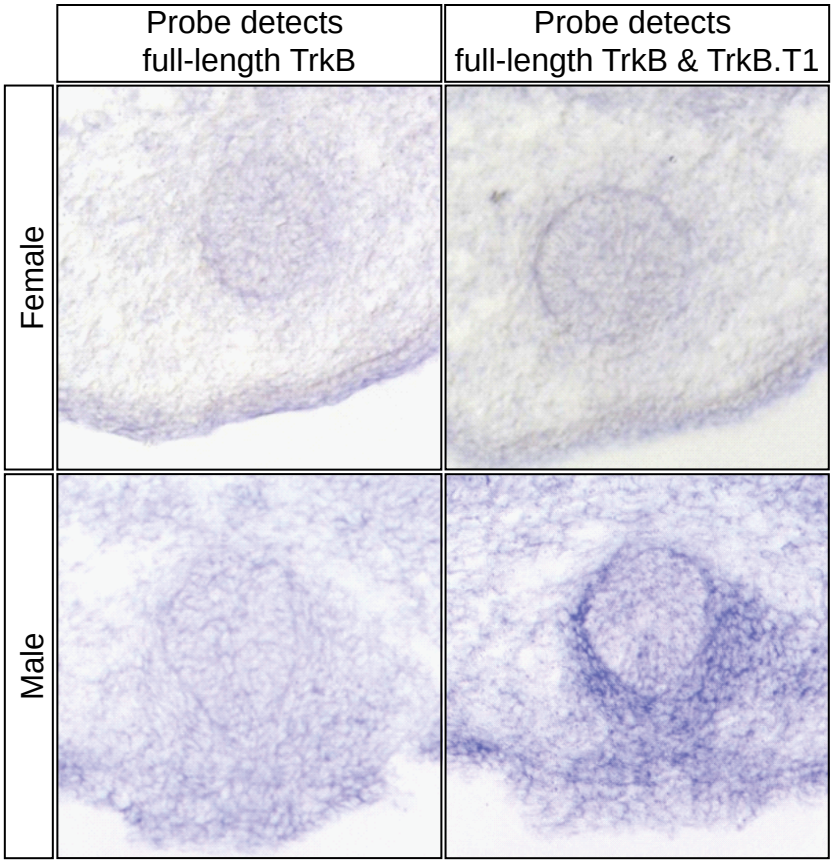

Fig. S13. The truncated form of TrkB is the only form of TrkB transcript expressed in the E13 wildtype male mammary mesenchyme. *In situ* hybridization of mammary gland sections of male and female late E13 embryos using two different TrkB probes. The probe that detects full-length TrkB recognizes the 3' UTR of full-length TrkB transcript; the probe that detects both forms recognizes sequences encoding the extracellular domain of TrkB. Note that there is no full-length transcript detected either in male or female mammary mesenchyme at this stage. All experiments were done at least three times with similar findings.

Fig. S14

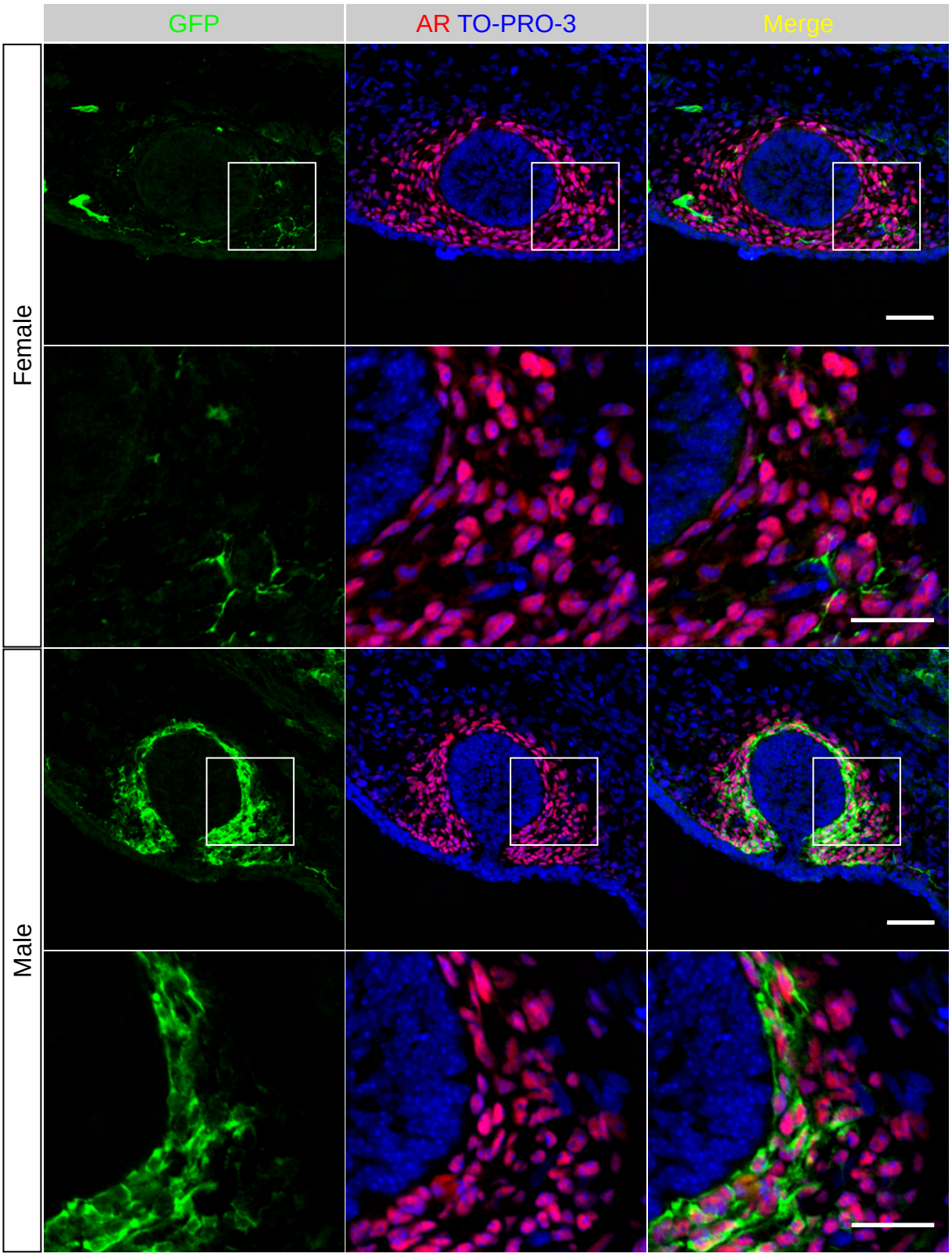

Fig. S14. TrkB and the androgen receptor are co-expressed in a large subset of E13 male mammary mesenchymal cells. *TrkB*$^{GFP/+}$ embryos were obtained at late E13, and sections of both male and female rudimentary mammary glands were stained with anti-GFP, anti-AR, and TO-PRO-3. Pictures were taken by confocal microscopy by acquiring 1-μm optical images through the middle of the sections. Note that GFP is expressed in androgen receptor expressing mammary mesenchymal cells in the male but not the female. This experiment was done three times with similar results. Scale bar: 50μm for original pictures, 25 μm for the cropped panels.

Fig. S15

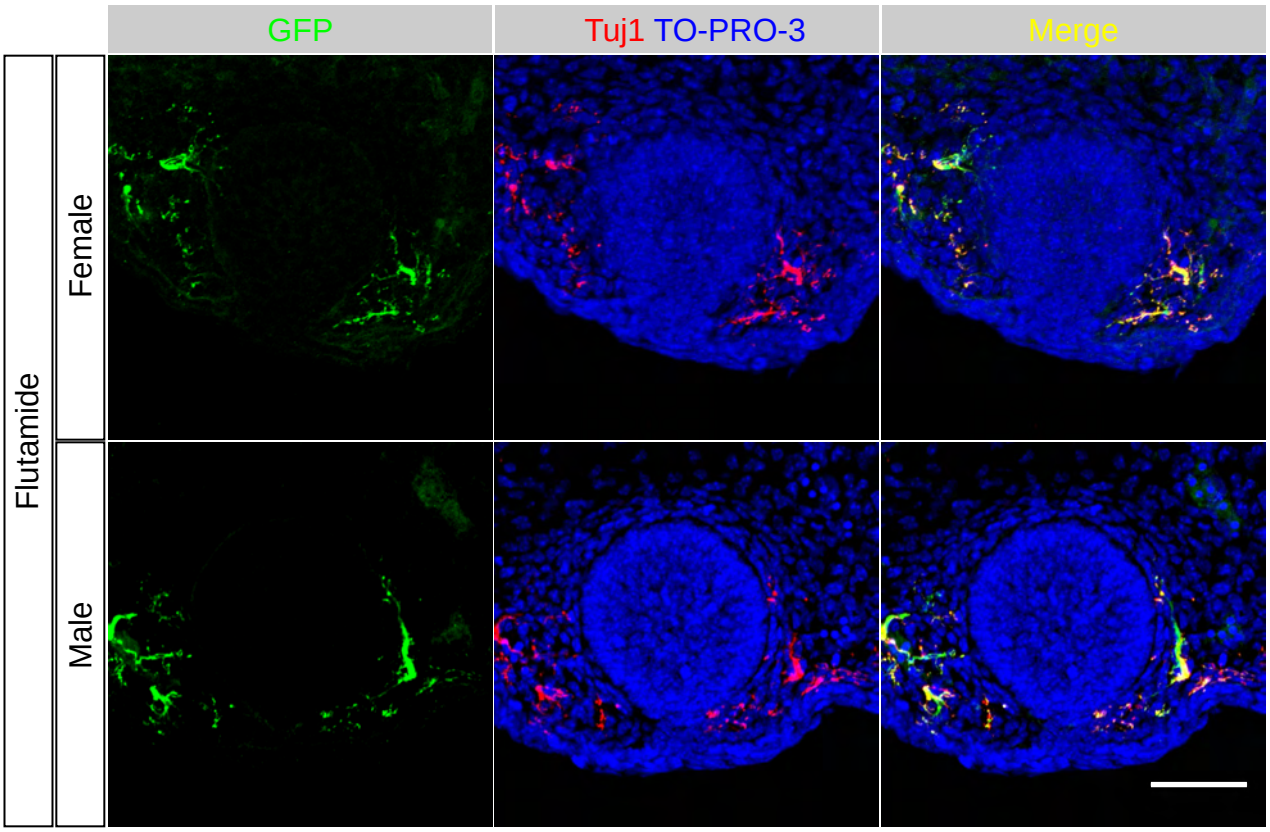

Fig. S15. Androgens regulate mesenchymal TrkB expression at the transcriptional level. Pregnant dams crossed with *TrkB*$^{GFP/+}$ males were treated with flutamide beginning at late E12. Embryos were collected at late E13, and mammary gland sections were stained with anti-GFP, anti-Tuj1, and TO-PRO-3. Note that GFP expression was not detected in mammary mesenchymal cells of the flutamide treated male embryos. This experiment was done two times with similar results. Scale bar: 50μm.

Fig. S16

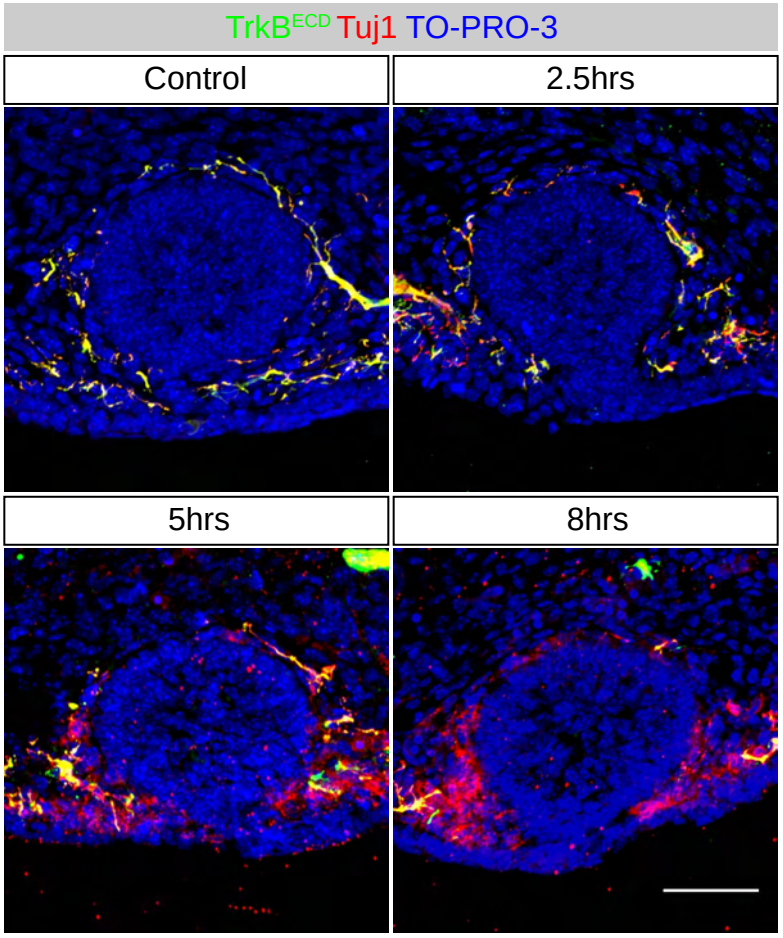
TrkB^ECD Tuj1 TO-PRO-3
Control
2.5hrs
5hrs
8hrs

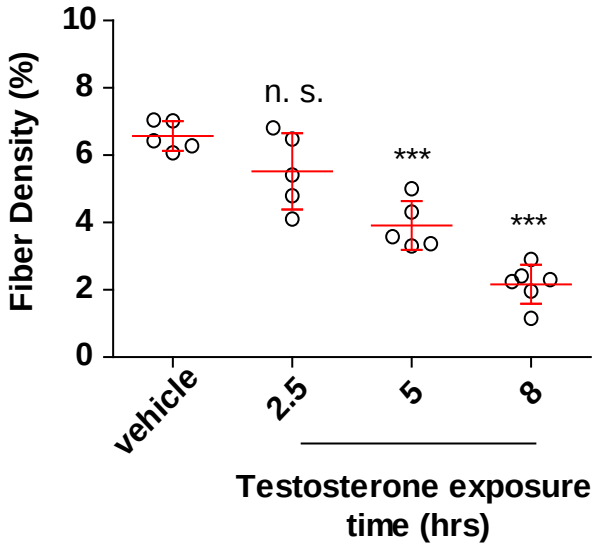
Fiber Density (%)
10
8
6
4
2
0
n. s.
***
***
vehicle
2.5
5
8
Testosterone exposure time (hrs)

Fig. S16. TrkB expression in female mammary mesenchyme after testosterone exposure. $TrkB^{ECD}$ and Tuj1 staining of mammary gland sections from female embryos that were treated with testosterone for the indicated times. All embryos were collected at late E13. In the quantification plot, each dot represents the average fiber density of the ten mammary glands of one embryo (red lines: means ± standard deviation, statistical analysis was done using one-way ANOVA, and data for each time point is compared with the control group). Scale bar: 50μm.

Fig. S17

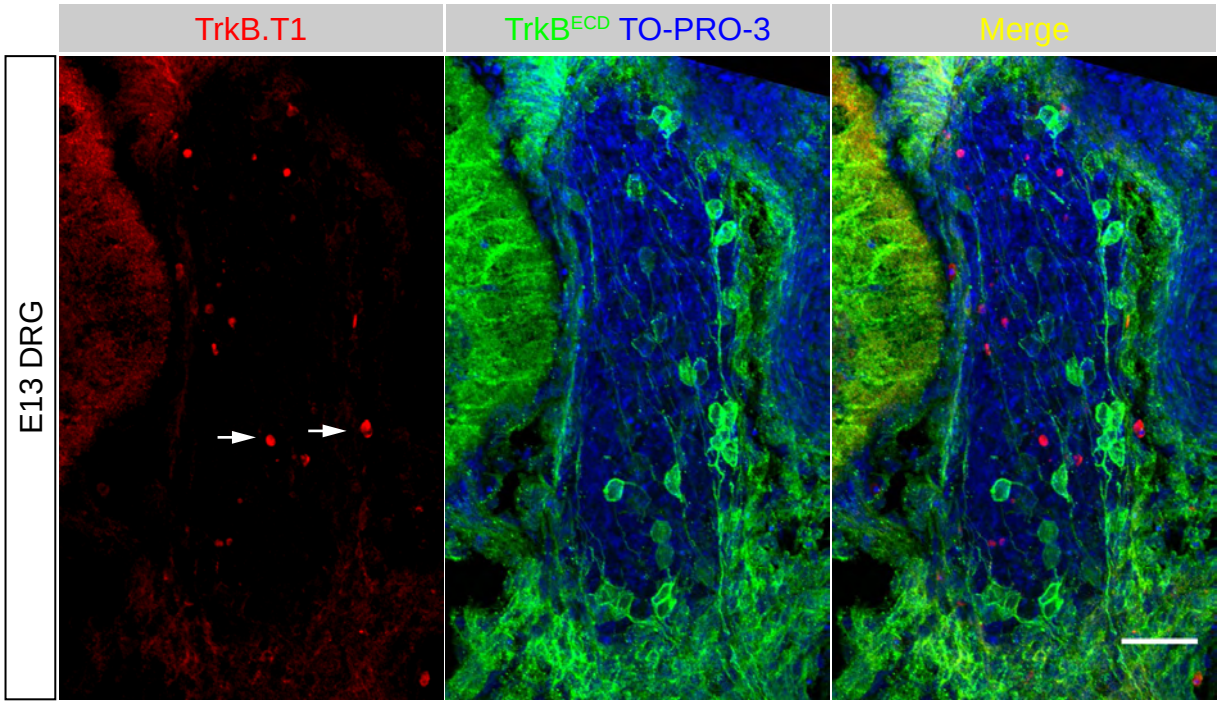

Fig. S17. The truncated form of TrkB is undetectable in DRG neurons at E13. An E13 male DRG section was stained with the truncated form-specific TrkB antibody, and co-stained with anti-TrkB^{ECD} and TO-PRO-3. The sparse staining observed using the truncated form-specific TrkB antibody within the DRG is due to non-specific antibody binding to blood cells (arrows). This experiment was done three times with similar results. Scale bar: 50µm.

Fig. S18

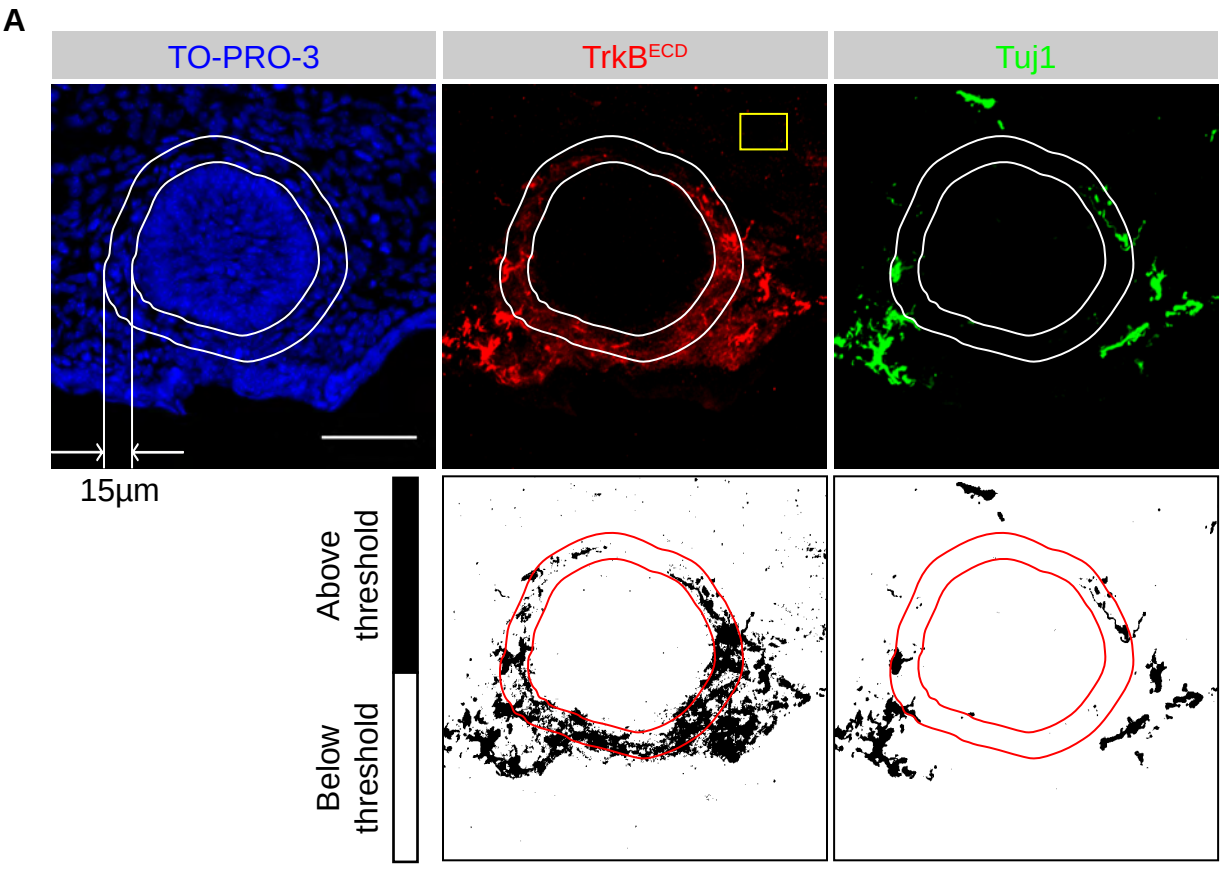

$$\text{mean } F_{TrkB} = \text{mean } F_{TrkBot} - \text{mean } F_{background}$$

$$S_{TrkB} = S_{TrkBot} - S_{Tuj1ot}$$

$$\Sigma F_{TrkB} = \text{mean } F_{TrkB} \times S_{TrkB}$$

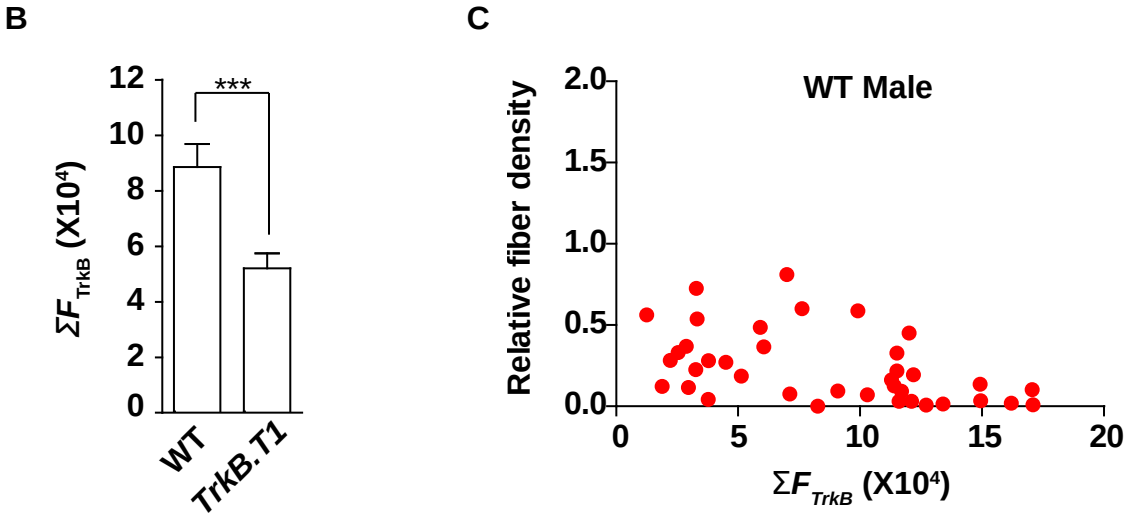

Fig. S18. Quantification of mammary mesenchymal TrkB expression levels. (**A**) All images were taken using a Zeiss LSM700 Laser scanning confocal microscope. The scanning gain was determined by adjusting the fluorescence intensity of $TrkB^{ECD}$ staining of neuronal fibers to saturation. All images were processed using ImageJ software. The threshold was determined using the default setting in ImageJ, and the average mammary mesenchymal $TrkB^{ECD}$ staining fluorescence intensity (mean F_{TrkB}) is calculated as the average fluorescence intensity of over-threshold pixels (mean F_{TrkBot}, avoiding TrkB and Tuj1 double positive pixels) within the 15μm band minus the average background fluorescence intensity (mean $F_{background}$, within the yellow square in the image shown). The area of mesenchymal $TrkB^{ECD}$ staining (S_{TrkB} is defined as the area of over-threshold pixels of $TrkB^{ECD}$ staining (S_{TrkBot}) minus the area of over-threshold pixels of Tuj1 staining (S_{Tuj1ot}) within the 15 μm band. The total mesenchymal TrkB level ($\sum F_{TrkB}$) is defined as the mean F_{TrkB} multiplied by S_{TrkB}. (**B**) Quantification of mammary mesenchymal TrkB level in wildtype and *TrkB.T1* mutant male embryos at late E13. (**C**) The relationship between the total mammary mesenchymal TrkB level and the relative fiber density of individual mammary glands of wildtype male embryos (correlation coefficient: r=-0.4893, p=0.0016, 38 glands from 5 mice). Scale bar: 50μm.

Fig. S19

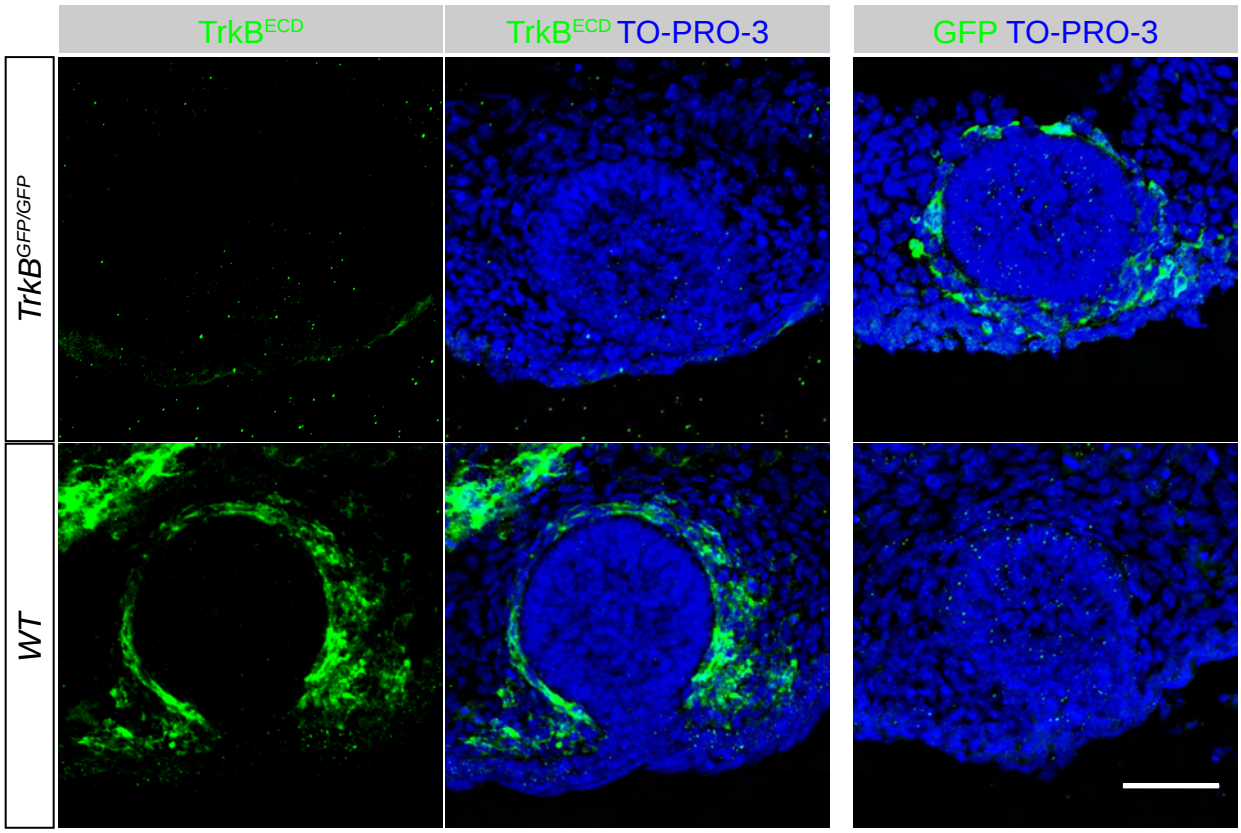

Fig. S19. Assessment of TrkB^{ECD} antibody specificity. Mammary gland sections of late E13 *TrkB$^{GFP/GFP}$* and wildtype male embryos were immunostained using the TrkB^{ECD} antibody and TO-PRO-3 or the GFP antibody and TO-PRO-3. This experiment was done two times with similar results. Scale bar: 50µm.

Fig. S20

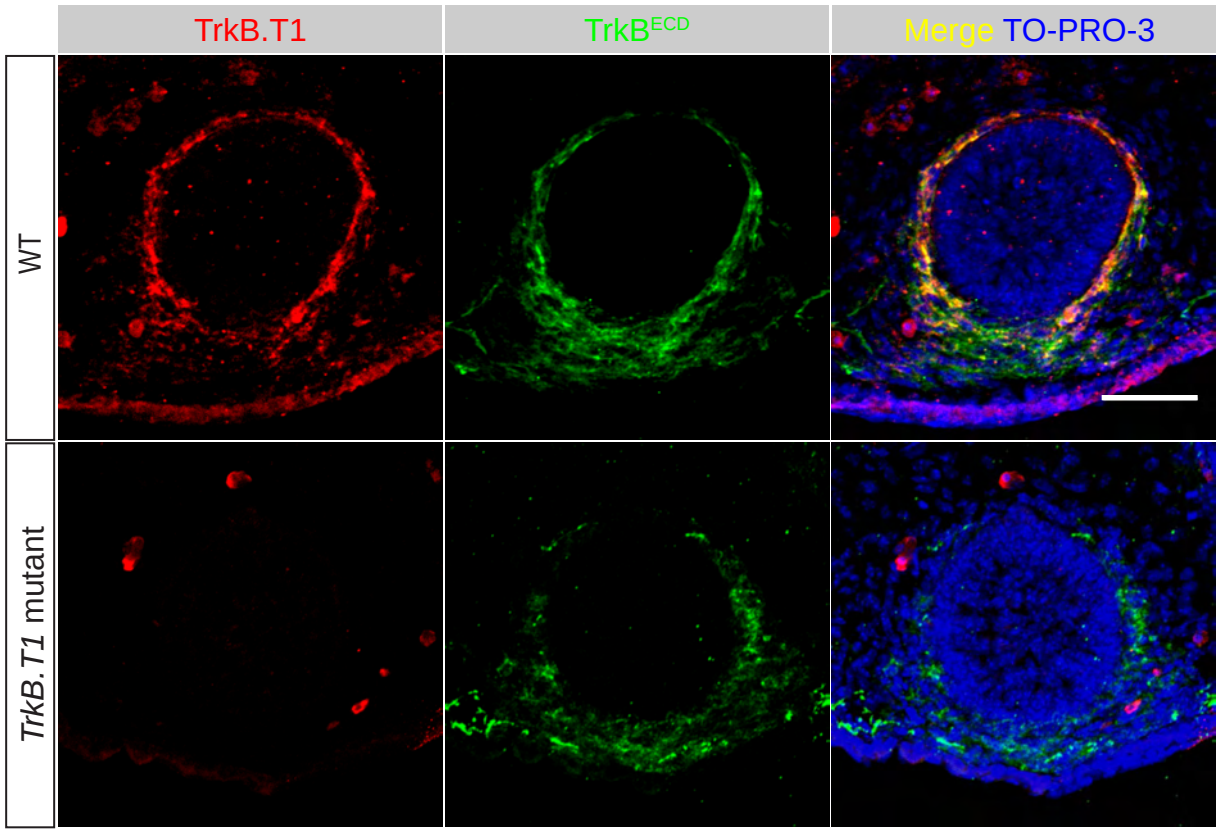

Fig. S20. The residual TrkB detected in mammary mesenchymal cells of *TrkB.T1* mutant male embryos lacks the TrkB.T1 specific c-terminus. Mammary gland sections of late E13 wildtype and *TrkB.T1* mutant males were stained using the truncated form-specific TrkB antibody, the TrkB^{ECD} antibody and TO-PRO-3. The residual TrkB expressed in the mutant and recognized by the TrkB^{ECD} antibody cannot be detected by the truncated form-specific TrkB antibody. This experiment was done two times with similar results. Scale bar: 50μm.

Fig. S21

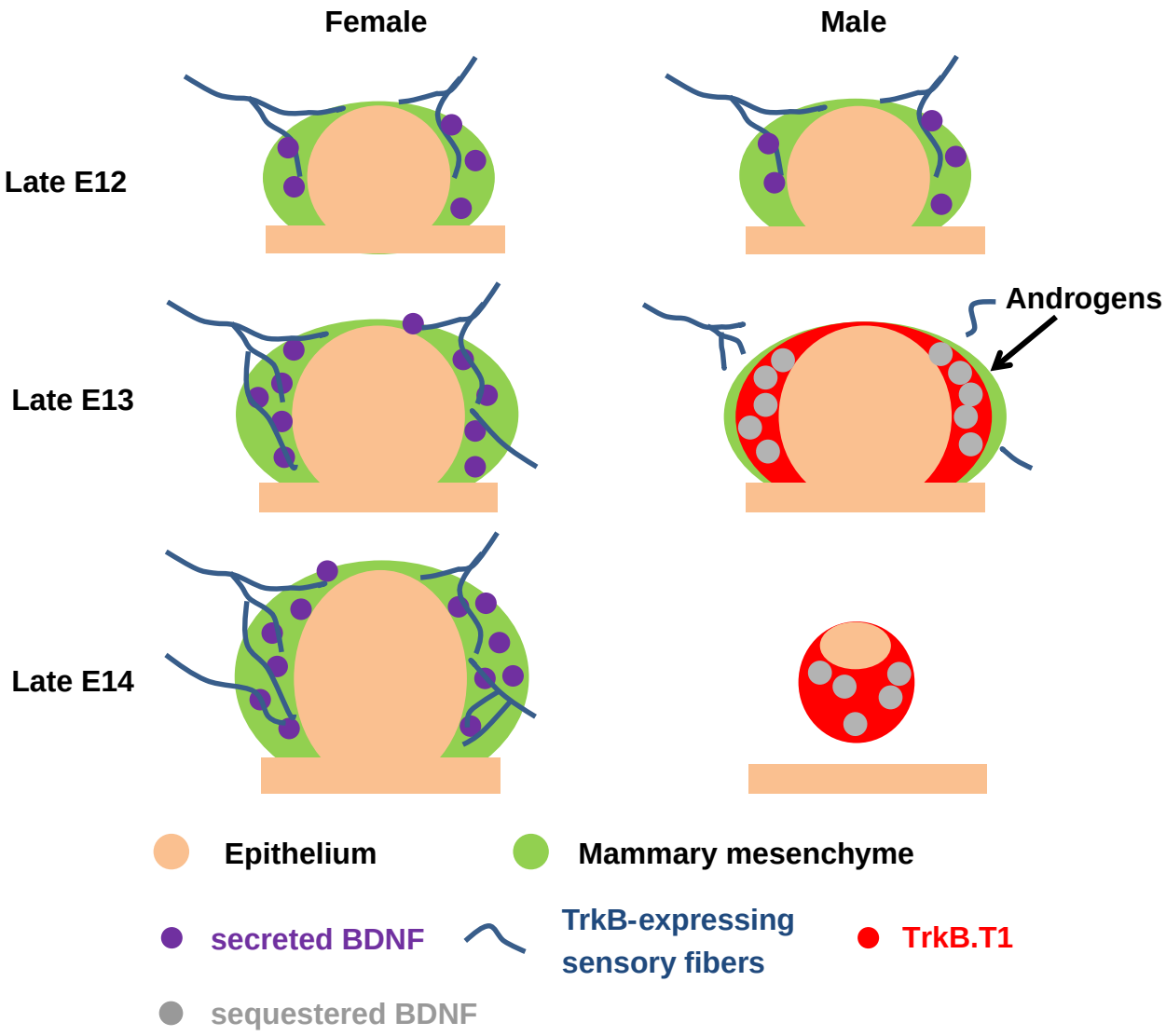

Fig. S21. Schematic illustration of the cellular and molecular mechanism by which sexually dimorphic mammary gland sensory innervation is generated. BDNF produced in both male and female mammary mesenchymal cells promotes initial ingrowth and maintenance of TrkB-dependent sensory fibers. Then, beginning at E13, androgens released by male gonads and acting upon receptors in male mammary mesenchymal cells trigger robust expression of the truncated form of TrkB, which neutralizes BDNF–TrkB signaling, leading to rapid pruning of sensory fibers associated with male glands. Thus, a sex hormone-dependent switch in BDNF–TrkB signaling generates the sexually dimorphic pattern of rudimentary mammary gland sensory innervation.

References

1. G. W. Robinson, Cooperation of signalling pathways in embryonic mammary gland development. *Nat. Rev. Genet.* **8**, 963 (2007).

2. M. E. Dunbar *et al*., Parathyroid hormone-related protein signaling is necessary for sexual dimorphism during embryonic mammary development. *Development* **126**, 3485 (1999).

3. E. J. Nordeen, K. W. Nordeen, D. R. Sengelaub, A. P. Arnold, Androgens prevent normally occurring cell death in a sexually dimorphic spinal nucleus. *Science* **229**, 671 (1985).

4. L. L. Wright, A. J. Smolen, The role of neuron death in the development of the gender difference in the number of neurons in the rat superior cervical ganglion. *Int. J. Dev. Neurosci.* **5**, 305 (1987).

5. R. B. Simerly, Wired for reproduction: Organization and development of sexually dimorphic circuits in the mammalian forebrain. *Annu. Rev. Neurosci.* **25**, 507 (2002).

6. J. A. Morris, C. L. Jordan, S. M. Breedlove, Sexual differentiation of the vertebrate nervous system. *Nat. Neurosci.* **7**, 1034 (2004).

7. N. G. Forger, Cell death and sexual differentiation of the nervous system. *Neuroscience* **138**, 929 (2006).

8. L. K. Low, H. J. Cheng, Axon pruning: An essential step underlying the developmental plasticity of neuronal connections. *Philos. Trans. R. Soc. Lond. B Biol. Sci.* **361**, 1531 (2006).

9. T. D. Patel, A. Jackman, F. L. Rice, J. Kucera, W. D. Snider, Development of sensory neurons in the absence of NGF/TrkA signaling in vivo. *Neuron* **25**, 345 (2000).

10. M. F. Lyon, S. G. Hawkes, X-linked gene for testicular feminization in the mouse. *Nature* **227**, 1217 (1970).

11. M. Bibel, Y. A. Barde, Neurotrophins: Key regulators of cell fate and cell shape in the vertebrate nervous system. *Genes Dev.* **14**, 2919 (2000).

12. E. J. Huang, L. F. Reichardt, Neurotrophins: Roles in neuronal development and function. *Annu. Rev. Neurosci.* **24**, 677 (2001).

13. L. Li *et al*., The functional organization of cutaneous low-threshold mechanosensory neurons. *Cell* **147**, 1615 (2011).

14. X. Chen *et al*., A chemical-genetic approach to studying neurotrophin signaling. *Neuron* **46**, 13 (2005).

15. R. Klein, L. F. Parada, F. Coulier, M. Barbacid, trkB, a novel tyrosine protein kinase receptor expressed during mouse neural development. *EMBO J.* **8**, 3701 (1989).

16. J. K. Atwal, B. Massie, F. D. Miller, D. R. Kaplan, The TrkB-Shc site signals neuronal survival and local axon growth via MEK and P13-kinase. *Neuron* **27**, 265 (2000).

17. R. Klein, D. Conway, L. F. Parada, M. Barbacid, The trkB tyrosine protein kinase gene codes for a second neurogenic receptor that lacks the catalytic kinase domain. *Cell* **61**, 647 (1990).

18. S. Biffo, N. Offenhäuser, B. D. Carter, Y. A. Barde, Selective binding and internalisation by truncated receptors restrict the availability of BDNF during development. *Development* **121**, 2461 (1995).

19. R. H. Fryer, D. R. Kaplan, L. F. Kromer, Truncated trkB receptors on nonneuronal cells inhibit BDNF-induced neurite outgrowth in vitro. *Exp. Neurol.* **148**, 616 (1997).

20. S. G. Dorsey *et al*., In vivo restoration of physiological levels of truncated TrkB.T1 receptor rescues neuronal cell death in a trisomic mouse model. *Neuron* **51**, 21 (2006).

21. J. A. Gorski, S. R. Zeiler, S. Tamowski, K. R. Jones, Brain-derived neurotrophic factor is required for the maintenance of cortical dendrites. *J. Neurosci.* **23**, 6856 (2003).

22. S. da Silva *et al*., Proper formation of whisker barrelettes requires periphery-derived Smad4-dependent TGF-beta signaling. *Proc. Natl. Acad. Sci. U.S.A.* **108**, 3395 (2011).

23. M. H. Kaufman, *The Atlas of Mouse Development* (Academic Press, San Diego, CA, 1992).

24. A. C. Bishop *et al*., A chemical switch for inhibitor-sensitive alleles of any protein kinase. *Nature* **407**, 395 (2000).

25. W. Luo *et al*., A hierarchical NGF signaling cascade controls Ret-dependent and Ret-independent events during development of nonpeptidergic DRG neurons. *Neuron* **54**, 739 (2007).

26. Q. Liu *et al*., Molecular genetic visualization of a rare subset of unmyelinated sensory neurons that may detect gentle touch. *Nat. Neurosci.* **10**, 946 (2007).

27. S. O. Mueller, J. A. Clark, P. H. Myers, K. S. Korach, Mammary gland development in adult mice requires epithelial and stromal estrogen receptor alpha. *Endocrinology* **143**, 2357 (2002).

28. H. Hasegawa, S. Abbott, B. X. Han, Y. Qi, F. Wang, Analyzing somatosensory axon projections with the sensory neuron-specific *Advillin* gene. *J. Neurosci.* **27**, 14404 (2007).

29. L. Madisen *et al*., A robust and high-throughput Cre reporting and characterization system for the whole mouse brain. *Nat. Neurosci.* **13**, 133 (2010).

30. I. Fariñas, K. R. Jones, C. Backus, X. Y. Wang, L. F. Reichardt, Severe sensory and sympathetic deficits in mice lacking neurotrophin-3. *Nature* **369**, 658 (1994).